2nd URSI AT-RASC, Gran Canaria, 28 May – 1 June 2018

Field Trials for Ultrawideband Antenna

I. Farhat[(1)], D. Cutajar[(1)], K. Zarb Adami[(1)(2)(3)], and C. Sammut[(3)]
(1) Institute of Space Sciences and Astronomy, University of Malta, Malta,
(2) University of Oxford, United Kingdom
(3) Department of Physics. University of Malta, Malta

Abstract

A beam pattern verification system in real operating conditions is essential to illustrate the performance and technical challenges of a proposed radio entity. It is key to high-accuracy cosmological and astronomical measurements. For future application on a verification system based on a proposed tightly coupled array, operating from 300 MHz to 1 GHz, a characterization system based on a flying far-field source implementation on an ultrawideband log-periodic antenna is verified in this communication. The far-field flying source is based on a commercially-available unmanned remotely operated Octocopter, equipped with a differential GNSS to determine the sampling point positions. The proposed setup has been validated at 750 MHz and found to be in good agreement with a full-wave prediction. At this stage, the resulting 2D beam pattern flying source characterization shows promising results for ongoing and future aperture array radio astronomy experiments.

1 Introduction

The pre-construction phase of a radio telescope necessitates the establishment of a verification system that can verify that a candidate design meet functionality specification, cost target, and site requirement. In this framework, the radiation pattern verification system is necessary for the development of the instrument. Because of the large size of radio subarrays and long distance required to satisfy far-field conditions, this characterization activity cannot be conducted in anechoic chambers or outdoors elevated test ranges. Unlike indoors beam pattern measurements, field trails evaluation method takes into account environment effect.

Drone-based radio calibration setup was presented in [1] for 21 cm instruments. Previous works on the UAV-mounted calibration source verification system [1], [2] have shown excellent results for single antenna pattern measurements in the frequency range between 150 and 408 MHz. The first application on the accuracy of antenna response modeling was for the Square Kilometre Array (SKA) [3] low stations was on an array pattern of a small 3 $\times$ 3 dual-polarization Vivaldi antennas [4]. Then the system upgraded as a phase calibrator in [5] at 408 MHz. Also, beam pattern measurements of a 16-element linear dual-polarized log-periodic test array, designed to meet SKA-low instrumentation requirements, using UAV-validating system was reported in [6]. Full beam map of a 5 m dish telescope was demonstrated in [7].

This paper reports on a successful characterization of a single antenna at 750 MHz for future implementation on a proposed tightly coupled phased array [8] for SKA-MFAA (300 MHz to 1 GHz). In this method, the radiation pattern is calculated from a post-processing procedure which has both the received power at the antenna port and the UAV position data as inputs.

The paper is organized as follows: in Section 2, UAV-beam pattern characterization system is discussed. Section 3 describes the experimental results for log-periodic 2D beam pattern. Section 4 concludes the paper.

2 Beam Characterization System

The field trail instrumentation setup used in this experiment is classified into three sectors; far-field flying source, receiving system and data post-processing. The flying far-field source consists of a commercial Octocopter [9] equipped with a transmitting dipole (operating at 750 MHz) via a continuous wave RF-signal generator, see Figure 1. For the construction of the beam pattern of the Antenna Under Test (AUT), the radiation pattern of the flying source was considered performing a full-wave electromagnetic simulation using the commercial software Ansoft HFSS v12 [10]. The on-ground receiving system (AUT) is a commercially available log-periodic broadband yagi antenna(Figure 2), operating over frequencies from 700 MHz to 6 GHz, located 20 m from a spectrum analyzer. The measurement was triggered by virtue of a MATLAB [11] script every second (each time)which recorded the amplitude of the received signal from the output of a low noise amplifier(LNA) with a gain of about 29 dB (to compensate for the subsequent coaxial cable attenuation). The MATLAB script utilizes the NI-VISA API installed on the computer connected to the spectrum analyzer.

For a centimetric tracking of the UAV position during the flight, a dual-GNSS module is co-located on the copter. The

Figure 1. Octocopter-mounted sky source.

Figure 2. AUT.

differential-GNSS is based on two C94-M8P boards each integrated with an NEO-M8P-2 module, one with moving baseline and the other with rover functionality. The 3D position of the drone is streamed through the rover to a PC (Intel stick PC), using MATLAB statements. In this case, the rover position solution provides the user with a vector describing the difference between the base and rover locations.

Planar quasi-grid pattern flight measurements have been performed in the principal plane $\phi = 0$ (South-North (SN) direction) with a constant height of 30 m and the AUT is at the center of the reference system. After take-off, the UAV is switched to follow an autonomous GPS-guided flight according to a pre-programmed path, which corresponds to E-plane cut. The flight time duration is just enough to allow for one complete path per flight, following which, the batteries would require replacement.

All sampled data from the rover and spectrum analyzer are synchronized to the PC clock, such that the signal from the spectrum analyzer is matched at every time-instant to the drone location in the sky when this signal was emitted. Then, the synced data is linearly interpolated over the gaps in the signal. In this way, the received power pattern of the overall system, along with the UAV flying path, can be easily constructed.

3 2D Beam Pattern

The measurement system is based on the far-field two antenna method, the flying far-field transmitting dipole, and the AUT, which employs the Friis transmission formula [12]. It is paramount that the distance between the two antennas, i.e. the altitude of the copter, is kept constant such that the far-field criteria is satisfied [12].

$$\text{Far-Field} \geq \frac{2D^2}{\lambda} \tag{1}$$

where D represents the antenna dimensions (length or diameter of the antenna), f the signal frequency, and λ the wavelength. For flying far-field source under far-field approximation, the gain of the AUT is described by [1], [2] as

$$G_{AUT}(\hat{r}).M(\hat{r}) = \frac{P_R(\underline{r})}{G_s(\hat{r},\alpha,\beta,\gamma)P_S G_R}.\left(\frac{4\pi R}{\lambda}\right)^2 \tag{2}$$

where $G_{AUT}(\hat{r})$ is the gain of the AUT in spherical reference identified by $\hat{r}$ unit vector, $M(\hat{r})$ is polarization mismatch, P_R the measured received power at AUT port, $\underline{r}$ is the position vector from the AUT to the test source, $G_s(\hat{r},\alpha,\beta,\gamma)$ the source radiation pattern (The angles α , β and γ are bearing, pitch and roll which describe the UAV orientation measured by on board inertial measurement unit (IMU), P_S the source transmitted power and G_R is the LNA gain and cable losses [2]. Friis formula can be written in a logarithmic decibel form as

$$\begin{aligned} G_{AUT}(dB) =& P_R(dB) - G_s(dB) - 20\log\left(\frac{\lambda}{4\pi R}\right) - G_R(dB) \\ & - P_s(dB) \end{aligned} \tag{3}$$

Hence, the AUT pattern is obtained by removing the simulated contribution of the source pattern $G_s(\hat{r},\alpha,\beta,\gamma)$, the path loss and the quantities P_S and G_R from the measured received power P_R.

The received power pattern of the quasi-rectangular scan along the co-polar of the AUT results is reported in Figure 3. The flight pattern was designed to cover a grid of $30\,m \times 30\,m$. The grid is oriented such that roughly most of the tracks would pass through the extent of the main beam.

After calibrating a number of 10 flying paths that formulate the gridded path, a 2D plane information of the beam

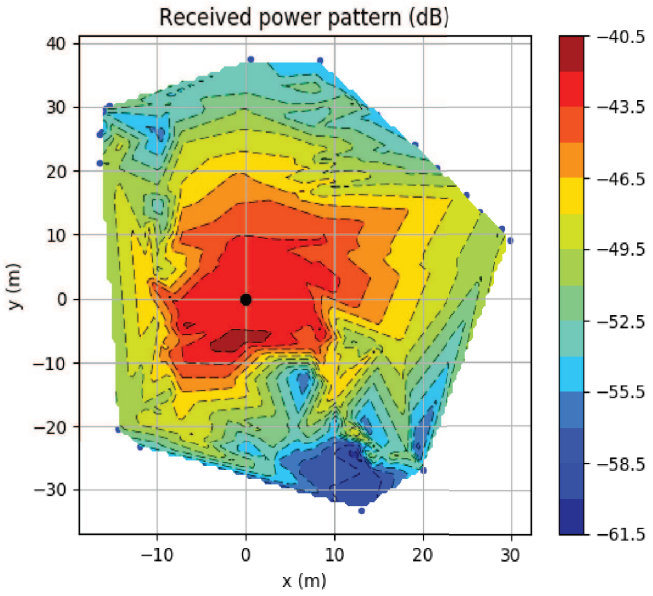

Figure 3. Received power pattern from the front-end of the AUT at 750|MHz.

is formed on the grid. Further information on the 2D beam pattern is realized by interpolating this plane using a post-processing python script. Figure 3 illustrates extracted E-plane pattern at zenith. A curve fitting technique was used to find the best estimate of E-plane cut at the zenith. In order to examine and assess the accuracy of the measurements, the measured beam pattern was compared with full-wave simulations of the AUT. The E-plane pattern comparison results Figure 4 show a good agreement. However, this technique is still under development and further improvements are to be integrated into the system in order to achieve a map of a full beam pattern measurement.

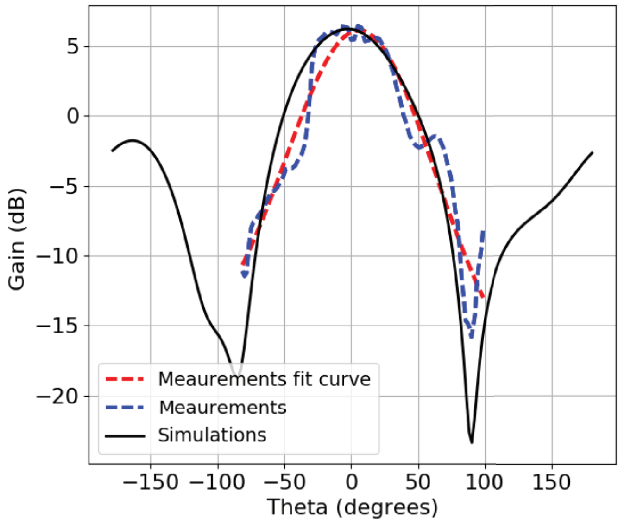

Figure 4. Measured co-polar (dashed, and simulated cross polar (solid) in the E plane.

4 Conclusion

In this letter, preliminary results of a UAV beam pattern characterization system at 750 MHz is reported. For an ultrawideband log-periodic antenna, field trial beam pattern evaluation results show a reasonable accuracy for the co-polar plane. Further improvement for a proper formulation to extract the AUT radiation pattern from the received power pattern is considered in future work. Overall, the experimental measurements show promising results and validate the system which can be adopted for phased array measurements and calibration.

References

[1] A. Virone, G., M. Lingua, M.and Piras, A. Cina F. Perini, J. Monari, F. Paonessa, O. A. Peverini, A. Giuseppe, and R. Tascone, "Antenna pattern verification system based on a micro unmanned aerial vehicle (uav)," in *IEEE Antennas and Wireless propagation Letters*, vol. 13, 2014, pp. 169–172.

[2] G. Virone, F. Paonessa, O. A. Peverini, G. Addamo, O. R., and R. Tascone, "Antenna pattern measurements with a flying far-field source (hexacopter)," in *IEEE Conference on Antenna Measurements Applications (CAMA)*, vol. 57, 2014, pp. 1–2.

[3] P. E. Dewdney, P. Hall, R. Schilizzi, and T. Lazio, "The square kiliometer array," *Proc. IEEE*, vol. 97, pp. 1482–1496, June 2009.

[4] G. Virone *et al.*, "Uav-based radiation pattern verification for a small low-frequency array,," in *2014 IEEE Antennas and Propagation Society International Symposium (APSURSI)*, 2014, pp. 995–996.

[5] G. Pupillo *et al.*, "Medicina array demonstrator: calibration and radiation pattern characterization using a uav-mounted radio-frequency source,," *Experimental Astronomy*, pp. 405–421, 2015.

[6] C. Chang, C. Monstein, A. Refreqier, A. Amara, A. Glauser, and S. Casura, "Beam calibration of radio telescopes with drones,," *astei-ph-IM*, pp. 1–12, 2015.

[7] E. de Lera Acedo *et al.*, "Ska aperture array verification system: Electromagnetic modeling and beam pattern measurements using a micro uav,," *rXiv:1703.00537 [astro-ph.IM]*, pp. 1–18, 2016.

[8] I. Farhat, K. Zarb Adami, J. Abelal, and C. Sammut, "Genetic algorithm application on a tightly coupled array antenna,," in *2017 11th European Conference on Antennas and Propagation (EUCAP)*, 2017, pp. 2281–2285.

[9] http://wiki.mikrokopter.de/en/ArfOktoXL.

[10] http://www.ansys.com/products/electronics/ansys-hfss. [Online]. Available: https://www.ansys.com/

[11] MATLAB. (2015) http:www.matchworks.com.

[12] C. A. Balanis, *Antenna Theory: Analysis and Design*. New Jersey: John Wiley Sons, 2005, ch. 12.